Acta Cryst. (1997). D**53**, 160–168

X-ray Structure of the 154-Amino-Acid Form of Recombinant Human Basic Fibroblast Growth Factor. Comparison with the Truncated 146-Amino-Acid Form

JETTE SANDHOLM KASTRUP,[a]* ELISABETH SAUER ERIKSSON,[b] HENRIK DALBØGE[c] AND HANS FLODGAARD[d]†

[a]*PharmaBiotec Research Center, Department of Medicinal Chemistry, Royal Danish School of Pharmacy, Universitetsparken 2, DK-2100 Copenhagen Ø, Denmark,* [b]*Department of Molecular Biology, Uppsala Biomedical Center, Uppsala University, S-751 24 Uppsala, Sweden, and Institute of Molecular Biology and Howard Hughes Medical Institute, University of Oregon, Eugene, OR 97403, USA,* [c]*Symbion, Novo Nordisk A/S, Fruebjergvej 3, DK-2100 Copenhagen Ø, Denmark, and* [d]*Health Care Research, Bioscience, Novo Nordisk A/S, Novo Alle, DK-2880 Bagsvaerd, Denmark. E.-mail: kastrup@medchem.dfh.dk*

(Received 9 May 1996; accepted 11 October 1996)

Abstract

The crystal structure of the 154-amino-acid form of human basic fibroblast growth factor (hbFGF154), probably representing the intact form of hbFGF as deduced from the open reading frame of hbFGF cDNA, was determined by X-ray crystallography and refined to a crystallographic residual of 19.0% for all data between 20.0 and 2.0 Å resolution. Crystals were obtained from recombinant hbFGF154 expressed in *E. coli*. hbFGF154 has the same overall structure as the N-terminus truncated 146-amino-acid form. The structure has a Kunitz-type fold and is built of 12 β-strands of which six antiparallel strands form a β-sheet barrel. In the structure it was possible to locate two additional residues at the N terminus and the last three C-terminal amino-acid residues, which seem to be disordered in all but one of the reported structures of the truncated form of hbFGF. The C-terminal amino-acid residues are part of the last β-strand through the formation of a hydrogen bond between the main-chain amide group of Ala152 and the carbonyl O atom of Pro28. An apparent phosphate ion is bound within the basic region on the surface of the molecule and has as ligands the side chains of Asn35, Arg128 and Lys133 and two water molecules. A slightly different hydrogen-bonding pattern to the phosphate ion is observed as compared with the sulfate ions in the truncated forms [Eriksson, Cousens & Matthews (1993). *Protein Sci.* **2**, 1274–1284; Zhang, Cousens, Barr & Sprang (1991). *Proc. Natl Acad. Sci. USA*, **88**, 3446–3450]. One molecule of β-mercaptoethanol forms a disulfide bridge to Cys77.

1. Introduction

Basic fibroblast growth factor (bFGF) is a member of a family of proteins which stimulate the proliferation and differentiation of a variety of cell types (Burgess & Maciag, 1989; Whitman & Melton, 1989) through the receptor-mediated pathways (Dionne *et al.*, 1990; Lee, Johnson, Cousens, Fried & Williams, 1989). It induces mitogenic and chemotactic activity, and is a potent mediator of wound healing, angiogenesis and neural outgrowth (Benharroch & Birnhaum, 1990; Burgess & Maciag, 1989; Folkman & Klagsbrun, 1987; Gospodarowicz, Ferrara, Schweigerer & Neufeld, 1987; Walicke, Cowan, Ueno, Baird & Guillemin, 1986).

The FGF family (Baird & Klagsbrun, 1991) comprises eight known members which all have a strong affinity for heparin, and the proteins are also referred to as heparin-binding growth factors (HBGF's) (Finch, Rubin, Miki, Ron & Aaronson, 1989; Lobb, Harper & Fett, 1986; Marics *et al.*, 1989). Heparin has been shown to modify the activity of hbFGF (Uhlrich, Lagente, Lenfant & Courtois, 1986; Neufeld, Gospodarowicz, Dodge & Fujii, 1987) and to protect it from acid inactivation (Gospodarowicz & Cheng, 1986) and from proteolytic digestion (Baird, Schubert, Ling & Guillemin, 1988; Saksela, Moscatelli, Sommer & Rifkin, 1988). Growth stimulation by hbFGF requires not only interaction with the hbFGF cell-surface receptor, but also the presence of heparan sulfate proteoglycans which can bind to both hbFGF (Yayon, Klagsbrun, Esko, Leder & Ornitz, 1991; Sakaguchi, Yanagishita, Takeuchi & Aurbach, 1991; Klagsburn & Baird, 1991) and to the hbFGF receptor (Kan *et al.*, 1993).

Determination of the true molecular weight of bFGF has been complicated by the susceptibility of the protein to protease-mediated truncation at the amino terminus during purification, which however, has no adverse effect on the biological activity (Gospodarowicz *et al.*, 1985, 1986; Ueno, Baird, Esch, Ling & Guillemin, 1986; Klagsbrun *et al.*, 1987). When first sequenced, bFGF was reported to be a 146-amino-acid polypeptide (Esch *et al.*, 1985). However, a 154-amino-acid form of bFGF, extended at the amino terminus by eight amino acids, was isolated from pituitary and brain, when purified in the presence of protease inhibitors (Ueno *et*

ISSN 0907-4449

al., 1986; Klagsbrun *et al.*, 1987). A 154-amino-acid form of bFGF is consistent with the open reading frame of bFGF cDNA (Abraham, Wang, Tumolo, Mergia & Fiddes, 1986) and probably represents the intact form of bFGF. Reports exist of even longer forms of bFGF (Florkiewicz & Sommer, 1989; Prats *et al.*, 1989).

Three-dimensional structures of two types of the amino-terminus truncated 146-amino-acid form of human bFGF (hbFGF146) have been determined by X-ray crystallography, the wild type (Ago, Kitagawa, Fujishima, Matsuura & Katsube, 1991; Eriksson, Cousens, Weaver & Matthews, 1991; Eriksson *et al.*, 1993; Faham, Hileman, Fromm, Linhardt & Rees, 1996; Ornitz *et al.*, 1995; Zhang *et al.*, 1991) and a serine mutant (Ago *et al.*, 1991; Zhu *et al.*, 1991). Here, we report the refined three-dimensional structure of the 154-amino-acid form of hbFGF (hbFGF154) determined by X-ray crystallography using recombinant hbFGF expressed in *E. coli*.

2. Experimental

2.1. *Expression and purification*

A synthetic gene encoding Met-hbFGF (155 amino acids) was constructed on the basis of the published amino-acid sequence (Abraham *et al.*, 1986). The correct hbFGF gene was isolated as a *ClaI*/*Eco*RI fragment and introduced into the expression vector pHD162SP9b (Dalbøge, Bayne, Christensen & Hejnaes, 1989). The resulting plasmid (pHD329) was expressed in *E. coli* MC1061 (Casadaban & Cohen, 1980) giving a yield of approximately 10 mg hbFGF (1 culture)$^{-1}$ $OD_{600=1}$.

The purification procedure was essentially as described for large-scale preparation by Iwane *et al.* (1987). As a final step the protein preparation was subjected to Mono-S fast protein liquid chromatography (Pharmacia, Sweden) and developed with a linear gradient from 0 to 1.0 *M* NaCl in 0.1 *M* sodium phosphate buffer pH 6.0. This procedure resulted in hbFGF154 with a purity greater than 95% as judged from SDS–PAGE (sodium dodecyl sulfate polyacrylamide gel electrophoresis). The protein solution was dialyzed against 20 m*M* 4-(2-hydroxyethyl)-piperazine-1-ethane-sulfonic acid (HEPES) buffer at pH 7.5 and concentrated to 10–15 mg ml^{-1} using centricon microconcentrators (Amicon, USA).

2.2. *Crystallization*

Crystallization of hbFGF154 was successful only by using polyethylene glycol (PEG) as precipitation agent, and the crystals suitable for X-ray structure determination were obtained from PEG 1000. The crystals were grown by the hanging-drop vapor-diffusion method (McPherson, 1982). 3–5 µl of hbFGF154 were mixed on siliconized cover slips with equal volumes of well solutions, typically 30–40% PEG 1000 and 0.2–0.3% β-mercaptoethanol (BME), and equilibrated at room temperature over 1 ml of well solution using a Linbro tissue-culture plate (Flow Laboratories Inc., USA). The reducing agent BME was essential for crystal growth and could not be substituted with dithiothreitol (DTT).

One crystal with the dimensions 0.05 × 0.10 × 0.15 mm was used for data collection. hbFGF154 crystallizes in space group *P*1 with one molecule per unit cell and cell dimensions of $a = 30.8$, $b = 33.3$, $c = 36.5$ Å, $\alpha = 64.1$, $\beta = 73.0$ and $\gamma = 76.1°$.

2.3. *Structure determination*

A 2.0 Å resolution diffraction data set was collected on a Xuong–Hamlin area detector (Xuong, Nielsen, Hamlin & Anderson, 1985; Hamlin, 1985) using graphite-monochromated Cu$K\alpha$ radiation with a Rigaku RU-200 rotating Cu-anode generator (40 kV, 150 mA) and processed using the data-reduction programs of Xuong *et al.* (1985). Only zero measurements were deleted, and Friedel pairs were averaged. The statistics of the final data set are shown in Table 1.

The structure was solved by difference Fourier using phases calculated from the 1.6 Å hbFGF146 structure (wt-Eriksson) determined by Eriksson *et al.* (1993). Initially, two cycles of rigid-body refinements were performed using the *TNT* refinement program package (Tronrud, Ten Eyck & Matthews, 1987; Tronrud, 1992) which reduced the crystallographic *R* value calculated for all reflections between 20.0 and 2.0 Å from 40.4 to 29.3%.

Least-squares refinements were performed with *TNT* alternating with graphics sessions using the program *O* (Jones, Bergdoll & Kjeldgaard, 1990). Occupancies of individual atoms were not refined. The *CCP*4 suite of programs (Collaborative Computational Project, Number 4, 1994) were used for calculation of unweighted electron-density maps. The *PROLSQ* program (Konnert & Hendrickson, 1980) from the *CCP*4 suite of programs was used for refinement of *B* values. Initially the individual *B* values were restrained to 20.0 Å^2 and were refined only in the last cycles of refinement. The *R* value for the final structure is 19.0%. The refinement statistics are given in Table 1.

Minor changes had to be made to the model of wt-Eriksson (amino-acid residues 28–151) to improve the agreement with the electron-density maps. Two additional N-terminal residues (Lys26, Asp27) and three C-terminal residues (Ala152, Lys153, Ser154) were located in the electron-density maps as refinements progressed. No interpretable density was observed for the first 25 N-terminal residues.

The *PEAKMAX* subroutine in the *CCP*4 suite of programs was used to define peaks in the difference maps (3σ cut-off level) particularly useful for locating

Table 1. *Statistics of the final data set and of the refinement*

The final data set	
Number of observations	15 506
with $I/\sigma_I < 1$	1404
$\geq 1, < 2$	2403
$\geq 2, < 5$	3825
≥ 5	7874
Total number of unique reflections (20.0–2.0 Å)	7035
Completeness to 2.0 Å (%)	84
Completeness between 2.4 and 2.2 Å (%)	93
Completeness between 2.2 and 2.0 Å (%)	47
$R_{sym}(F)$ $(I > 0\sigma)$	4.3
Refinement	
Maximum resolution (Å)	2.0
R value (%)	19.0
Number of atoms	1115
Protein atoms	1039
Water molecules	67
Phosphate	1
β-Mercaptoethanol	1
R.m.s. deviations from ideal geometry*	
Bond length (Å)	0.020
Bond angle (°)	2.7
Trigonal non-planarity (Å)	0.014
Planarity (Å)	0.018
Non-bonded contacts (Å)	0.022
Average B values (Å^2)†	
All atoms	22
All protein atoms	22
Main-chain atoms	20
Side-chain atoms	23
Water molecules	31
R.m.s. ΔB	2.0

*From the *TNT* program package. †Between covalently bonded atoms. B values were refined using *PROLSQ*.

water molecules. A water molecule was accepted, if the identified peak correlated with a separate peak in the corresponding $2|F_o| - |F_c|$ map, if one or more hydrogen bonds could be formed to atoms already present in the structure, and, if it was not too close (less than 2.3 Å) to any other atom.

The atomic coordinates and structure factors of the hbFGF154 structure have been deposited with the Protein Data Bank (Bernstein *et al.*, 1977).*

3. Results

3.1. *The final structure*

The structure of hbFGF154 consists of 12 antiparallel β-strands (Fig. 1) with a topology identical to a family of proteins with the Kunitz-type fold (McLachlan, 1979; Murzin, Lesk & Chothia, 1992). The structure includes one phosphate ion, one molecule of BME, and 67 water molecules six of which are buried within the hbFGF molecule. All water positions are stabilized by at least one hydrogen-bond interaction and the buried water molecules form at least two.

The final $2|F_o| - |F_c|$ map defines the structure of hbFGF154 well. The fit of the final structure in its electron density has been evaluated by real-space R values and rotamer side-chain fits (Jones, Zou, Cowan & Kjeldgaard, 1991) using the program *O* (Fig. 2). In addition, the individual B values of main-chain atoms and of side-chain atoms as a function of residue number

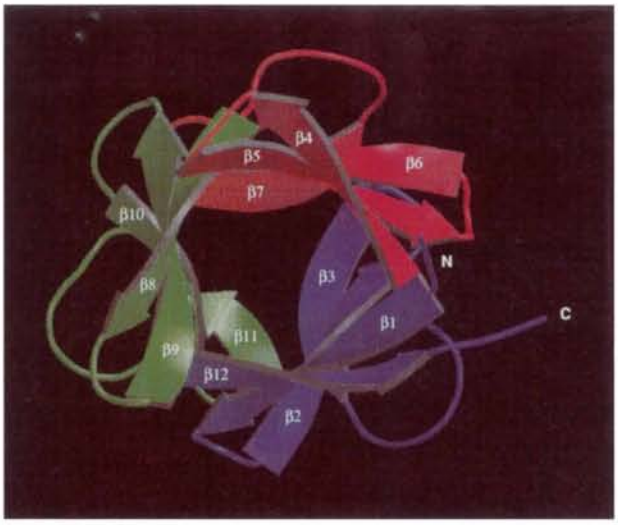

(*a*)

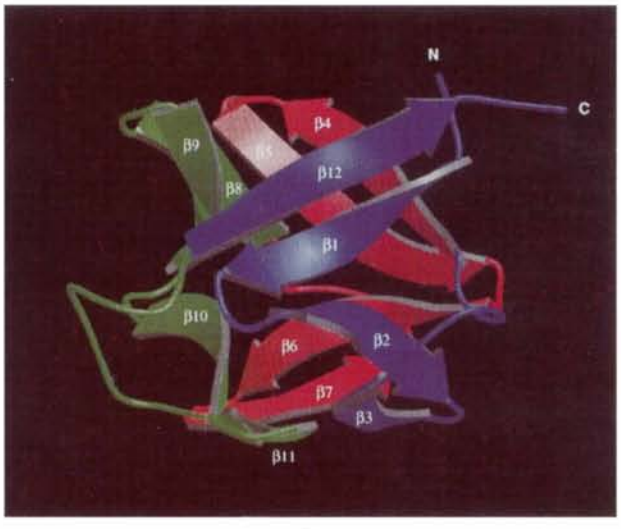

(*b*)

Fig. 1. Schematic picture of the β-trefoil fold of hbFGF154 (*a*) viewed along an axis of approximate threefold symmetry and (*b*) rotated 90°. Arrows represent β-strands and rattlers coils. (β1: 28–34, β2: 37–43, β3: 46–51, β4: 60–67, β5: 69–76, β6: 79–85, β7: 88–93, β8: 101–107, β9: 110–117, β10: 122–127, β11: 130–133, and β12: 146–152.)

*Atomic coordinates and structure factors have been deposited with the Protein Data Bank, Brookhaven National Laboratory (Reference: 1BFF, R1BFFSF). Free copies may be obtained through The Managing Editor, International Union of Crystallography, 5 Abbey Square, Chester CH1 2HU, England (Reference: LI0231).

Table 2. *R.m.s. deviations between the structures of hbFGF*

Residues 28–150 in hbFGF154 and residues 20–142 from the structures of the five truncated forms are included in the comparison. wt-Ago: 2.5 Å structure of wild-type hbFGF146 (Ago *et al.*, 1991); wt-Eriksson: 1.6 Å structure of wild-type hbFGF146 (Eriksson *et al.*, 1993); wt-Zhang: 1.8 Å structure of wild-type hbFGF146 (Zhang *et al.*, 1991); mt-Ago: 1.6 Å structure of (C69S, C87S) mutant of hbFGF146 (Ago *et al.*, 1991); mt-Zhu: 1.9 Å structure of (C69S, C87S) serine mutant of hbFGF146 (Zhu *et al.*, 1991).

	hbFGF154	wt-Ago	wt-Eriksson	wt-Zhang	mt-Ago	mt-Zhu
hbFGF154	—	1.55†	1.06†	1.58†	1.41†	1.05†
wt-Ago	0.32*	—	1.42†	1.82†	0.96†	0.99†
wt-Eriksson	0.29*	0.27*	—	1.48†	1.28†	0.91†
wt-Zhang	0.69*	0.64*	0.69*	—	1.68†	1.34†
mt-Ago	0.32*	0.14*	0.26*	0.63*	—	0.86†
mt-Zhu	0.29*	0.20*	0.25*	0.64*	0.18*	—

*R.m.s. deviations on main-chain atoms (C, Cα, N, O in Å). †R.m.s. deviations on side-chain atoms (Å).

are included in Fig. 2. The average real-space *R* value for the main-chain atoms is 8.7%. The largest values are observed for the N- and C-terminal residues and two surface loops. Regions with the highest real-space *R* values correlate with regions of highest *B* values. Overall the value distribution of the *B* factors are as can be expected from a protein structure. There are four residues with rotamer side-chain fits greater than 2.0 Å (Glu53, Glu86, Leu91 and Trp122). However, the electron density clearly defines those residues. There is one residue (Ser151) with deviating φ, ψ angles in the Ramachandran plot (not shown).

3.2. *Comparison with other hbFGF structures*

The hbFGF154 structure has been compared with five structures of the truncated forms of hbFGF deposited in the Protein Data Bank (*cf.* Table 2). R.m.s. deviations between hbFGF154 and the structure of wt-Eriksson are shown for all residues in Fig. 3.

All structures of hbFGF except for wt-Zhang show very small deviations with r.m.s values between 0.14 and 0.32 Å, superimposed on main-chain atoms only, and on side-chain atoms between 0.86 and 1.55 Å. Larger deviations (0.63–0.69 Å on main-chain atoms and 1.34–1.82 Å on side-chain atoms) are observed for wt-Zhang.

3.3. *The N- and C-terminal residues*

Compared to wt-Eriksson the position of five additional residues has been identified; Lys26 and Asp27 at the N-terminal end, and Ala152, Lys153 and Ser154 at the C-terminal end (Figs. 4*a*–4*c*). Lys26 and Asp27 are not part of the first β-strand structure. The distance between the main-chain Cα atoms of the last located residue (Lys26) towards the N-terminal and the C-terminal amino acid (Ser154) is 9.9 Å. Its main-chain O atom is situated 4.0 Å from the Nε2 atom of Gln62 and shows no close contact to other residues. The side chain of Asp27 is hydrogen bonded to a water molecule (2.3 Å).

The residues Ser151 and Ala152 at the C-terminal end form an extension of β-strand 12, the main-chain N atoms of Ala152 making a hydrogen bond to the main-chain O atom of Pro28 (3.3 Å) (*cf.* Fig. 4*c*). The main-chain O atom and the hydroxyl group of the side chain of Ser151 form hydrogen bonds to two water

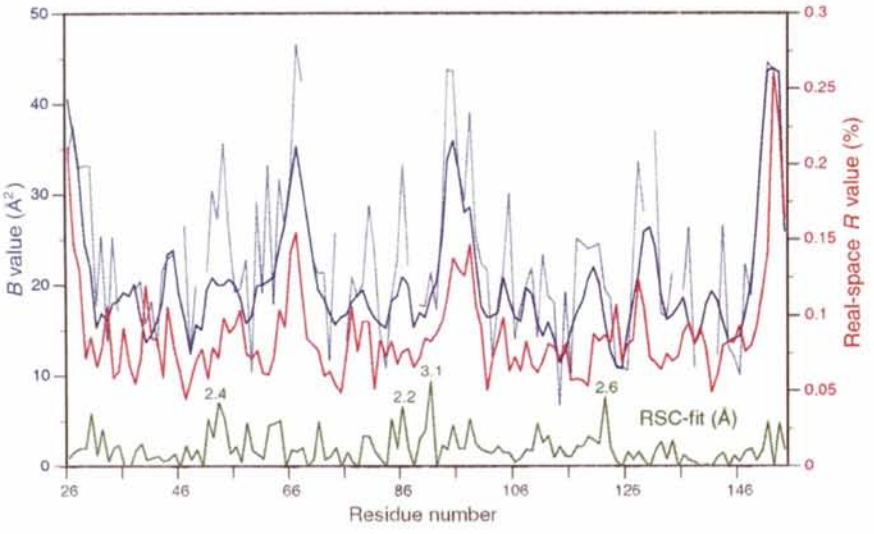

Fig. 2. The real-space *R* value (in %) for the main-chain atoms (red), the rotamer side-chain fits (in Å) (green), and the average temperature-factor values (in Å²) of the main-chain atoms (blue) and the side-chain atoms (dashed blue) of hbFGF154 as a function of the residue number.

molecules, 2.9 Å each. Ser151 adopts an unusual conformation ($\varphi = 111°$ and $\psi = -154°$). However, the electron density clearly suggests this conformation of Ser151 (*cf.* Figs. 4*a* and 4*b*), and forcing the residue into an allowed conformation leads to bad contacts with other residues. The side chain of Lys153 is well defined by the electron density. However, it shows no close contact to other amino acids, its side-chain Nζ atom is situated 8 Å from a symmetry-related molecule. The side-chain hydroxyl group of Ser154 forms weak contacts with the N$^{\zeta}$ atom of Lys34 (3.7 Å) and the N$^{\delta 2}$ atom of Asn109 (3.6 Å) of a symmetry-related molecule.

3.4. *The phosphate ion and the BME molecule*

An apparent phosphate ion is bound to the surface of the protein (Fig. 5). This part of the protein is generally basic with five of the 25 positively charged residues (Lys and Arg) situated within 5 Å from the phosphate ion. The hydrogen-bonding pattern to the O atoms of the phosphate ion involves three amino-acid residues (Asn35, Arg128 and Lys133) and two water molecules. The mean *B* value of the phosphate ion (37 Å^2) indicates some mobility of the ion.

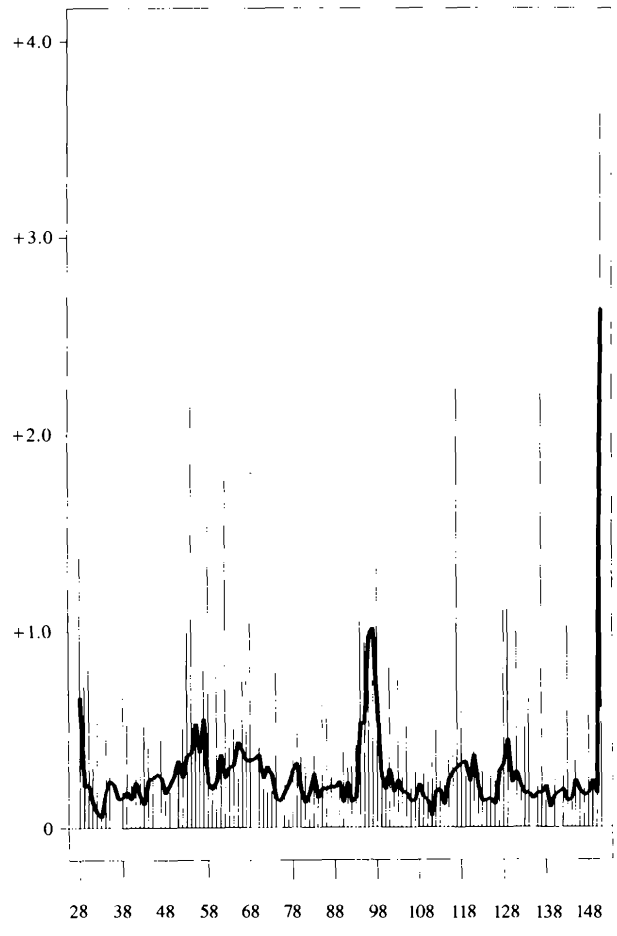

Fig. 3. R.m.s. deviations (Å) as a function of residue number of the main-chain atoms (continuous lines) and side-chain atoms (solid bars) between hbFGF154 and the truncated form of Eriksson *et al.* (1993). Superimposition was based on residues 28–151.

As in the structure of wt-Eriksson the electron density of the side chain of Arg128 is not perfectly defined. Two alternative conformations are suggested which both permit hydrogen bonds to the phosphate ion. In one conformation a single hydrogen bond is formed to the phosphate ion (not shown). When modelled in the second position two hydrogen bonds are formed by the guanido group (Fig. 5*b*) and the electron-density maps improve.

The thiol group of Cys77 forms a disulfide bridge to one BME molecule. The geometry is typical of a normal disulfide linkage, the distance between the two S atoms is 2.1 Å and the torsional angle Cys77—C$^{\beta}$—S$^{\gamma}$—S$^{\gamma}$—C$^{\beta}$—BME is −89°. The average *B* value for the BME molecule is 26 Å^2. The hydroxyl group of BME molecule forms a hydrogen bond (3.1 Å) to a water molecule and to one of the four O atoms of a phosphate ion bound to a symmetry-related protein molecule.

4. Discussion

The structure of the 154-amino-acid form of hbFGF, probably representing the intact form, is very similar to the structures of the eight-amino-acid truncated forms of hbFGF. This is in agreement with the observations that protease-mediated truncation at the amino terminus has no adverse effect on the biological activity. The largest r.m.s. deviations are observed to wt-Zhang which is crystallized in a different space group ($P2_12_12_1$) whereas all other structures have been crystallized in $P1$.

The largest differences between the hbFGF154 structure and the five truncated forms were observed in a loop region (Lys94–Asp98). In all available structures the *B* values of the main-chain atoms for these residues are relatively large and indicate structural flexibility within this region. The wt-Zhang structure shows large differences (2.32–2.45 Å) to all other structures in the loop region including Glu107–Asn110 (Glu99–Asn102 in hbFGF146). This loop region is very similar in all structures crystallized in $P1$ (0.10–0.27 Å). The difference might be explained by the fact that the main-chain N atom of Asn101 in wt-Zhang is hydrogen bonded to a symmetry-related sulfate ion not located in the other structures. Larger deviations are also observed for Ser151. In the structures of wt-Eriksson and mt-Zhu this is the last residue that could be located in the electron-density maps.

The irregular loop of hbFGF consisting of residues Arg177–Trp122, which is part of the putative

receptor-binding peptide identified by Baird *et al.* (1988), is similar in all structures but does not superimpose better than any other loop within the structure.

The positions of the buried water molecules and of 29 of the water molecules located at the surface of the hbFGF154 structure are almost identical to positions of water molecules located in the wt-Eriksson structure (*i.e.* with deviations of less than 1 Å and showing the same hydrogen-bonding pattern). The conservation of the buried water molecules suggests an important structural role.

In the wild-type structure wt-Ago the three last C-terminal residues also have been determined. The conformation of the C-terminal residues [Ser151 (143), Ala152 (144), Lys153 (145), Ser154 (146)] is different from that observed in the structure of hbFGF154 (Fig. 5*d*). However, their conformation also permits hydrogen bonding between Pro20 and Ala144 (3.1 Å) which corresponds to Pro28 and Ala152 in our structure. In

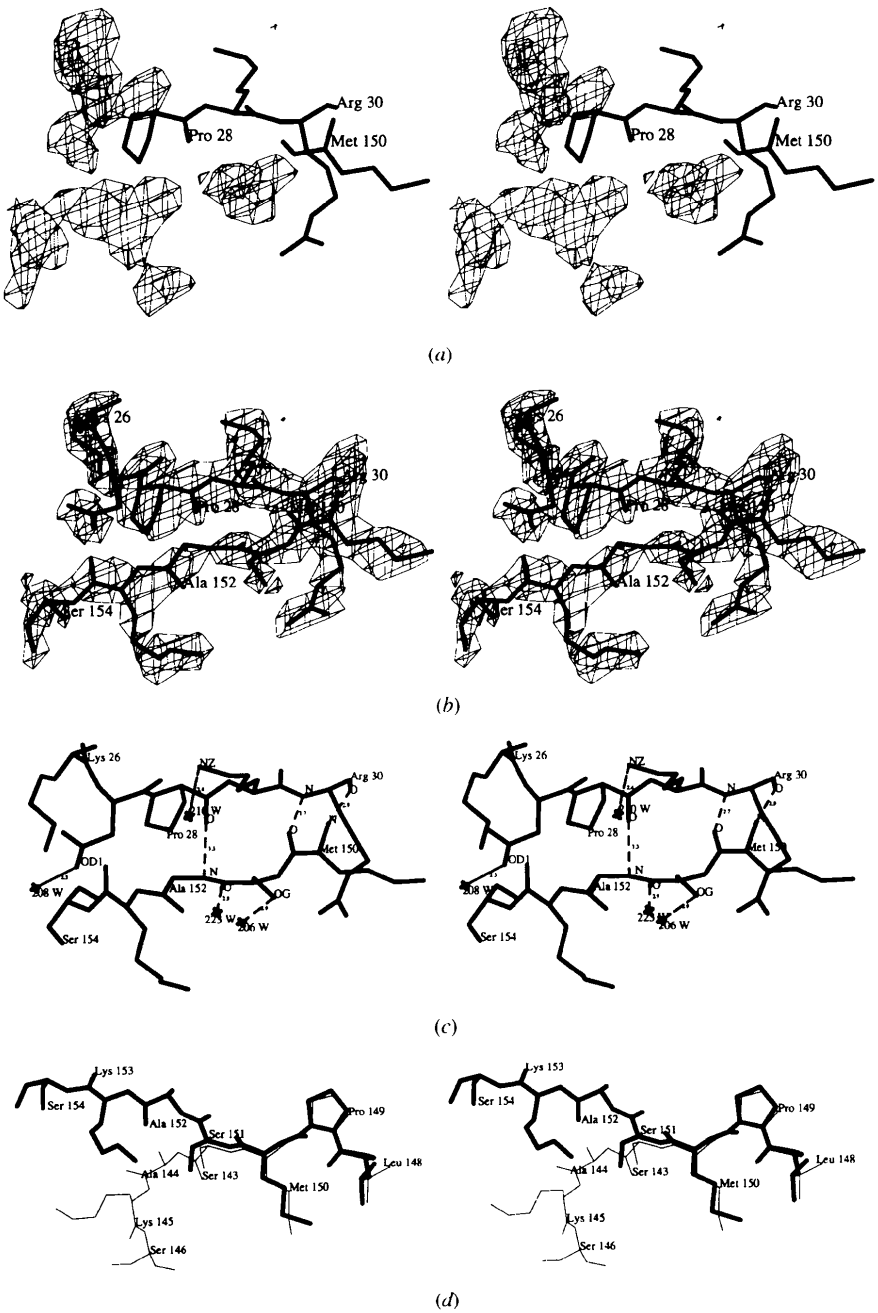

Fig. 4. (*a*) Difference Fourier map (*OMIT* map) in the C-terminal region after refinements without the residues Lys26, Asp27, Ser151, Ala152, Lys153 and Ser154. The view is identical to that of (*b*). Contours drawn at a level of 2.0σ where σ is the root-mean-square density throughout the unit cell. (*b*) Electron-density map ($2|F_o| - |F_c|$) in the vicinity of the N and C termini, superimposed on the refined structural model. Contours drawn at a level of 1.0σ. (*c*) Pattern of hydrogen bonds (dotted lines) in the vicinity of the N and C termini. (*d*) Comparison of the C terminus of hbFGF154 (thick lines) and of the truncated form of hbFGF of Ago *et al.* (1991) (thin lines).

both structures the *B* values of the main-chain atoms for the N-terminal and C-terminal residues are relatively high and no interpretable density was observed for the first 25 N-terminal residues which supports a high degree of flexibility. The eight-amino-acid extension in the full-length form as compared with the truncated form of hbFGF does not seem to lower the flexibility of the N-terminal residues.

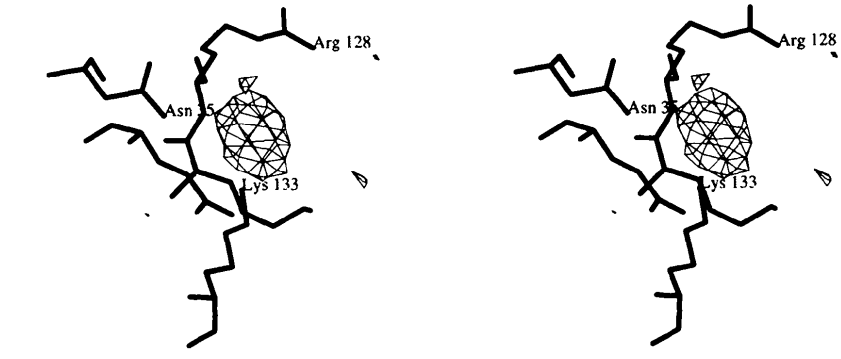

(*a*)

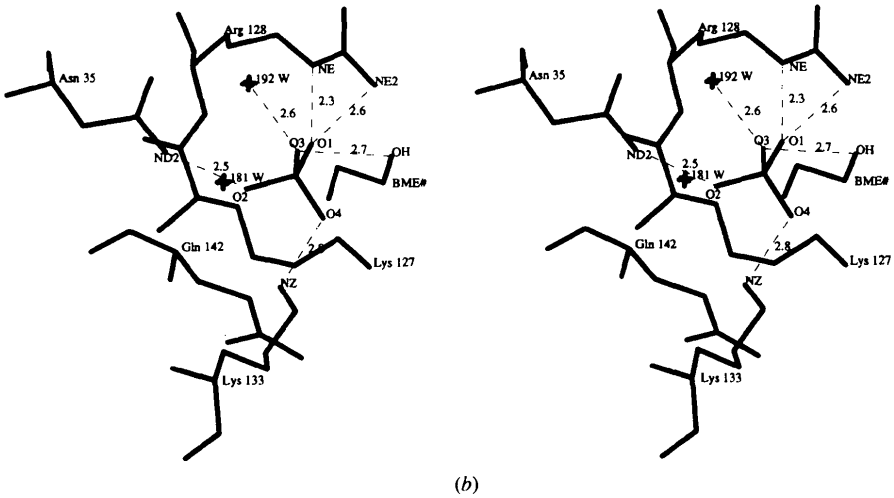

(*b*)

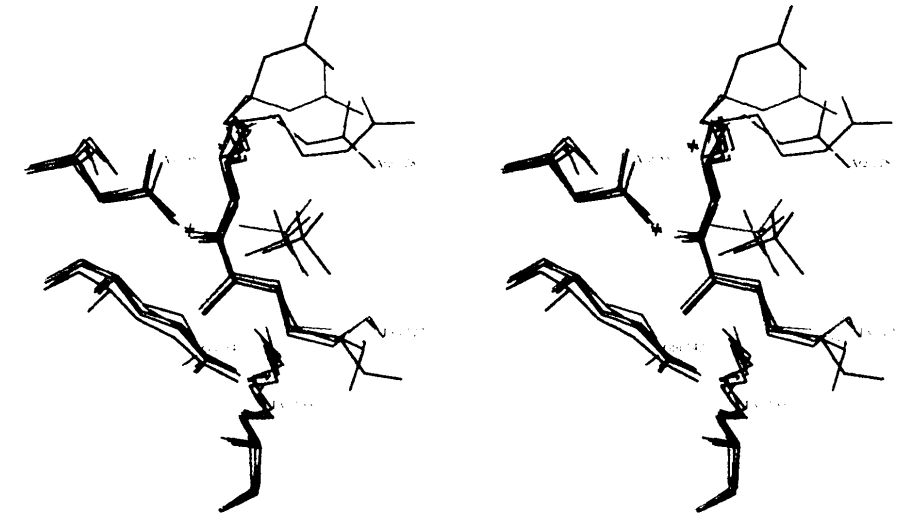

(*c*)

Fig. 5. (*a*) Difference Fourier map (*OMIT* map) at the phosphate-binding site after rigid-body refinements without any ion included. Contours drawn at a level of 3σ where σ is the root-mean-square density throughout the unit cell. (*b*) The phosphate-binding site in hbFGF154 showing the pattern of hydrogen bonds (less than 3.0 Å, dotted lines) to the phosphate ion and the corresponding distances. O3 also forms hydrogen bonds to the side-chain N^{ε} atom of Arg128 (3.1 Å) and to water 181 (3.1 Å). (*c*) A superimposition of the phosphate-binding site of hbFGF154 (red), the corresponding sulfate-binding site of wt-Eriksson (green) and wt-Zhang (blue), and wt-Ago (black), mt-Ago (yellow), and mt-Zhu (cyan).

A slightly different hydrogen-bonding pattern to the phosphate ion is observed as compared with the sulfate ion in wt-Eriksson, but in both structures the same three amino-acid residues [Asn35 (27), Arg128 (120) and Lys133 (125)] and two water molecules are forming hydrogen bonds to the O atoms of either the phosphate or the sulfate ions, respectively. The mean B value of the phosphate ion (37 Å^2) and the sulfate ion (46 Å^2), respectively, also indicate some mobility of the ions. Two sulfate ions were also observed at the same region in wt-Zhang, one forming hydrogen bonds to Asn35 (27) and Arg128 (120). However, in this structure Lys133 (125) is not involved in hydrogen bonding to the sulfate ions. By comparison of the different hbFGF structures it is evident that the side chain of Arg128 (120) shows a high degree of flexibility (Fig. 5*c*). In the truncated form of hbFGF the sulfate ion has been replaced by a selenate ion (Eriksson *et al.*, 1993) and one additional selenate ion was identified, hydrogen bonded to the side chains of Arg128 (120) and Lys133 (125) suggesting that both sites simultaneously contribute to the binding of heparin. In hbFGF154 no electron density was observed at the additional selenate ion site. Recent studies of Thompson, Pantoliano & Springer (1994) on hbFGF–heparin interactions by site-directed mutagenesis also establish Asn35 (27), Arg128 (120) and Lys133 (125) as very important for heparin binding, Lys133 being the single most important residue. Four X-ray crystal structures of complexes of hbFGF with two different non-sulfated saccharides (Ornitz *et al.*, 1995) and with two different heparin-derived saccharides (Faham *et al.*, 1996) also define a carbohydrate-binding site at the sulfate/phosphate ion binding site.

It is not likely that the phosphate ion could be a sulfate ion in this case as no sulfate had been included in either the purification or crystallization. However, during purification sodium phosphate buffers were used in concentrations up to 0.1 M. During crystallization HEPES was used as buffer in 20 mM concentrations and one might expect the binding site of the sulfonate group of a HEPES molecule at the sulfate ion binding site. However, the initial difference Fourier map (Fig 5*a*) and the final electron-density maps clearly indicate that this is not the case.

There are four cysteine residues in hbFGF (Cys33, Cys77, Cys95 and Cys100) of which Cys33 and Cys100 are highly conserved in the FGF family (Burgess & Maciag, 1989). hbFGF has appeared in multiple forms caused by sulfhydryl binding (Iwane *et al.*, 1987). hbFGF154 has a tendency to polymerize resulting in several oligomeric forms during storage. DTT does not prevent this polymerization in hbFGF154 and only after treatment with BME one band of monomeric hbFGF was observed on the SDS gel. Cys77, Cys95 and Cys100 are located at the surface of the molecule whereas Cys33 is buried within the protein molecule. A BME molecule is covalently bound to Cys77 (69) as in wt-Eriksson whereas the BME molecule bound to Cys100 (92) in wt-Eriksson is not apparent in the structure of hbFGF154. In the wild-type structure wt-Ago, where BME was also used during crystallization no bound BME molecules were located. However, the different numbers of BME molecules observed in the structures cannot be explained by the concentration of BME used, but might be a result of very different crystallization conditions.

We are grateful to H. Heinsøe for excellent technical assistance, E. B. Jørgensen for fermentation of the hbFGF154 production clone and T. Christensen for synthesis of the oligonucleotides, all from Novo Nordisk A/S, Denmark; Dr Michael Gajhede, University of Copenhagen, Denmark, and Dr Hanne Rasmussen, Royal Danish School of Pharmacy, Denmark for helpful assistance with the crystallography. JSK and ESE extend special thanks to Professor Brian W. Matthews and Dr Larry H. Weaver, University of Oregon, USA, for providing help and facilities for the data collection. The support of National Institutes of Health grant GM20066 to B. W. Matthews is also acknowledged. This work was supported by grants to JSK from the Alfred Benzons Foundation, and to ESE from the Swedish Natural Science Research Council. JSK also extends thanks to The PharmaBiotec Research Center and The Lundbeck Foundation.

References

Abraham, J. A., Wang, J. L., Tumolo, A., Mergia, A. & Fiddes, J. C. (1986). *CSH Symp. Quant. Biol.* **L1**, 657–667.

Ago, H., Kitagawa, Y., Fujishima, A., Matsuura, Y. & Katsube, Y. (1991). *J. Biochem.* **110**, 360–363.

Baird, A. & Klagsbrun, M. (1991). *Cancer Cells*, **3**, 239–244.

Baird, A., Schubert, D., Ling, N. & Guillemin, R. (1988). *Proc. Natl Acad. Sci. USA*, **85**, 2324–2328.

Benharroch, D. & Birnbaum, D. (1990). *Isr. J. Med. Sci.* **26**, 212–219.

Bernstein, F. C., Koetzle, T. F., Williams, G. J. B., Meyer, E. F. Jr, Brice, M. D., Rogers, J. R., Kennard, O., Shimanouchi, T. & Tasumi, M. (1977). *J. Mol. Biol.* **112**, 535–542.

Burgess, W. H. & Maciag, T. (1989). *Annu. Rev. Biochem.* **58**, 575–606.

Casadaban, J. M. & Cohen, S. N. (1980). *J. Mol. Biol.* **138**, 179–207.

Collaborative Computational Project, Number 4 (1994). *Acta Cryst.* D**50**, 760–763.

Dalbøge, H., Bayne, S., Christensen, T. & Hejnaes, K. R. (1989). *FEBS Lett.* **246**, 89–93.

Dionne, C. A., Crumley, G., Bellot, F., Kaplow, J. M., Searfoss, G., Ruta, M., Burgess, W. H., Jaye, M. & Schlessinger, J. (1990). *EMBO J.* **9**, 2685–2692.

Eriksson, A. E., Cousens, L. S. & Matthews, B. W. (1993). *Protein Sci.* **2**, 1274–1284.

Eriksson, A. E., Cousens, L. S., Weaver, L. H. & Matthews, B. W. (1991). *Proc. Natl Acad. Sci. USA*, **88**, 3441—3445.

Esch, F., Baird, A., Ling, N., Ueno, H., Hill, F., Denoroy, L., Klepper, R., Gospodarowitz, D., Boehlen, P. & Guillemin, R. (1985). *Proc. Natl Acad. Sci. USA*, **82**, 6507-6511.

Faham, S., Hileman, R. E., Fromm, J. R., Linhardt, R. J. & Rees, D. C. (1996). *Science*, **271**, 1116-1120.

Finch, P. W., Rubin, J. S., Miki, T., Ron, D. & Aaronson, S. A. (1989). *Science*, **245**, 752-755.

Florkiewicz, R. Z. & Sommer, A. (1989). *Proc. Natl Acad. Sci. USA*, **86**, 3978-3981.

Folkman, J. & Klagsbrun, M. (1987). *Science*, **235**, 442-447.

Gospodarowitz, D., Baird, A., Cheng, J., Lui, G. M., Esch, F. & Bohlen, P. (1986). *Endocrinology*, **118**, 82-90.

Gospodarowicz, D. & Cheng, J. (1986). *J. Cell. Physiol.* **128**, 475-484.

Gospodarowitz, D., Cheng, J., Lui, G. M., Fujii, D. K., Baird, A. & Bohlen, P. (1985). *Biochem. Biophys. Res. Commun.* **128**, 554-562.

Gospodarowitz, D., Ferrara, N., Schweigerer, L. & Neufeld, G. (1987). *Endocrinol. Rev.* **8**, 95-114.

Hamlin, R. (1985). *Methods Enzymol.* **114**, 416-452.

Iwane, M., Kurokawa, T., Sasada, R., Seno, M., Nakagawa, S. & Igarashi, K. (1987). *Biochem. Biophys. Res. Commun.* **146**, 470-477.

Jones, T. A., Bergdoll, M. & Kjeldgaard, M. (1990). In *Crystallographic and Modelling Methods in Molecular Design*, edited by C. Bugg & S. Ealick, pp. 189-199. New York: Springer-Verlag.

Jones, T. A., Zou, J.-Y., Cowan, S. W. & Kjeldgaard, M. (1991). *Acta Cryst.* A**47**, 110-119.

Kan, M., Wang, F., Xu, J., Crabb, J. W., Hou, J. & McKeehan, W. L (1993). *Science*, **259**, 1918-1921.

Klagsbrun, M. & Baird, A. (1991). *Cell*, **67**, 229-231.

Klagsbrun, M., Smith, S., Sullivan, R., Shing, Y., Davidson, S., Smith, J. A. & Sasse, J. (1987). *Proc. Natl Acad. Sci. USA*, **84**, 1839-1843.

Konnert, J. H. & Hendrickson, W. A. (1980). *Acta Cryst.* A**36**, 344-350.

Lee, P. L., Johnson, D. E., Cousens, L. S., Fried, V. A. & Williams, L. T. (1989). *Science*, **245**, 57-59.

Lobb, R. R., Harper, J. W. & Fett, J. W. (1986). *Anal. Biochem.* **154**, 1-14.

McLachlan, A. D. (1979). *J. Mol. Biol.* **133**, 557-563.

McPherson, A. J. (1982). *Preparation and Analysis of Protein Crystals*, pp. 82-160. New York: John Wiley.

Marics, I., Adelaide, J., Raybaud, F., Mattei, M.-G., Coulier, F., Planche, J., de Lapeyiere, O. & Birnbaum, D. (1989). *Oncogene*, **4**, 335-340.

Murzin, A. G., Lesk, A. M. & Chothia, C. (1992). *J. Mol. Biol.* **223**, 531-543.

Neufeld, G., Gospodarowicz, D., Dodge, L. & Fujii, D. K. (1987). *J. Cell. Physiol.* **131**, 131-140.

Ornitz, D. M., Herr, A. B., Nilsson, M., Westman, J., Svahn, C.-M. & Waksman, G. (1995). *Science*, **268**, 432-436.

Prats, H., Kaghad, M., Prats, A. C., Klagsbrun, M., Lelias, J. M., Liauzun, P., Chalon, P., Tauber, J. P., Amalric, F., Smith, J. A. & Caput, D. (1989). *Proc. Natl Acad. Sci. USA*, **86** 1836-1840.

Sakaguchi, K., Yanagishita, M., Takeuchi, Y. & Aurbach, G. D. (1991). *J. Biol. Chem.* **266**, 841-848.

Saksela, O., Moscatelli, D., Sommer, A. & Rifkin, D. B (1988). *J. Cell. Biol.* **107**, 743-751.

Thompson, L. D., Pantoliano, W. & Springer, B. A. (1994). *Biochemistry*, **33**, 3831-3840.

Tronrud, D. E. (1992). *Acta Cryst.* A**48**, 912-916.

Tronrud, D. E., Ten Eyck, L. F. & Matthews, B. W. (1987). *Acta Cryst.* A**43**, 489-503.

Ueno, N., Baird, A., Esch, F., Ling, N. & Guillemin, R. (1986). *Biochem. Biophys. Res. Commun.* **138**, 580-588.

Uhlrich, S., Lagente, O., Lenfant, M. & Courtois, Y. (1986). *Biochem. Biophys. Res. Commun.* **137**, 1205-1213.

Walicke, P., Cowan, M. W., Ueno, N., Baird, A. & Guillemin, R. (1986). *Proc. Natl Acad. Sci. USA*, **83**, 3012-3016.

Whitman, M. & Melton, D. A. (1989). *Ann. Rev. Cell Biol.* **5**, 93-117.

Yayon, A. Klagsbrun, M., Esko, J. D., Leder, P. & Ornitz, D. M. (1991). *Cell*, **64**, 841-848.

Xuong, N. H., Nielsen, C., Hamlin, R. & Anderson, D. (1985). *J. Appl. Cryst.* **181**, 342-350.

Zhang, J., Cousens, L. S., Barr, P. J. & Sprang, S. R. (1991). *Proc. Natl Acad. Sci. USA*, **88**, 3446-3450.

Zhu, X., Komiya, H., Chirino, A., Faham, S., Fox, G. M., Arakawa, T., Hsu, B. T. & Rees, D. C. (1991). *Science*, **251**, 90-93.